CHEMISTRY
A EUROPEAN JOURNAL

DOI: 10.1002/chem.201101650

Remarkably Selective Recognition of Iodobenzene Derivatives by a Macrocyclic Bis-Pt^{II} Metallohost

Robert Trokowski,[a] Shigehisa Akine,[a, b] and Tatsuya Nabeshima*[a, b]

Abstract: We designed and synthesized self-assembled bis-Pt^{II} dimer **1**·4 BF_4 with quino[8,7-*b*][1,10]phenanthroline as an extended π-face contact area, which acts as the first artificial receptor with high affinity toward iodinated aromatic compounds significantly based on noncovalent iodine···aromatic-plane interactions in a "side-on" fashion. Despite their structural similarity to a previously reported metallohost **2**$^{4+}$ that bears 2,2′:6′,2″-terpyridine units, a dramatic change in selectivity toward substituted benzene derivatives was observed for **1**$^{4+}$. ^{1}H NMR spectroscopic titration revealed a high affinity of **1**$^{4+}$ towards haloarenes, with exceptionally large association constants for 2-iodophenol ($K_a = 16000\,M^{-1}$) and 1,2-diiodobenzene ($K_a = 21000\,M^{-1}$), which are 93- and 140-fold higher, respectively, than the values obtained for **2**$^{4+}$. In addition, **1**$^{4+}$ showed a remarkably high affinity and selectivity toward 2,6-diiodophenol ($K_a = 35000\,M^{-1}$), which is an important substructure of the thyroid hormone T_4. X-ray crystallography and theoretical calculations strongly suggest that "side-on" iodine···aromatic-plane interactions and π–π stacking contribute to the strong 1,2-diiodobenzene and 2,6-diiodophenol binding. The results obtained here give unique and valuable insight into the nature of halogen atom interactions in their "side-on" region with an electropositive aromatic plane, which may provide useful guidance for designing artificial receptors for iodinated biomolecules.

Keywords: iodine · macrocycles · molecular recognition · platinum · self-assembly

Introduction

The appropriate combination of several noncovalent interactions, including halogen bonds,[1] can result in strong and precise molecular recognition. In particular, because of an anisotropic distribution of electron density around the halogen nucleus, iodine atoms in iodine-containing substances are able to participate in noncovalent interactions with electron-rich atoms or groups in a "head-on" way (Scheme 1) to form more efficient halogen bonding in artificial[2] and biological recognition systems[3] when compared to the other halogens. For example, I···O halogen-bonding and hydrophobic effects simultaneously contribute to the recognition of thyroid hormones by their specific receptors.[3a,d,e] Electron-deficient species such as protons of hydrogen-bond donors and metal ions can, on the other hand, also interact with halogen atoms in organic molecules to make C–X···H–C[4] and C–X···M^{n+} bonds[5,6] in which "side-on" interactions are often observed (Scheme 1). As hydrogen-bond acceptors, iodides and fluorides respectively form the weakest and strongest noncovalent C–X···H–C interactions among the halides. Although many examples of such hydrogen bonds and C–X···M^{n+} interactions have been reported, noncovalent "side-on" interactions between the electron-deficient aromatic plane and the electron-rich side periphery[7] of an iodine atom in iodinated compounds have rarely been investigated.[8] In these limited studies, "side-on" interactions between the iodine atoms and the aromatic surface of the metal complexes were suggested. However, the noncovalent interactions with the iodinated benzene derivatives were not elucidated clearly enough to enable application of the "side-on" interactions to the design of artificial receptors. We recently reported the quantitative synthesis and binding properties of self-assembled bis-Pt^{II} dimer **2**·4 BF_4,[9] which can act as a synthetic receptor because of its ability to selective-

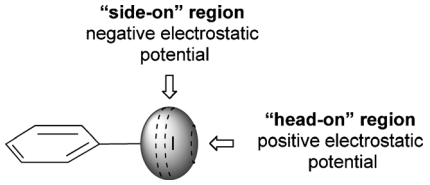

Scheme 1. The "side-on" and "head-on" interacting regions of the iodine atom in an iodoarene.

[a] Dr. R. Trokowski, Dr. S. Akine, Dr. T. Nabeshima
Graduate School of Pure and Applied Sciences
University of Tsukuba
1-1-1 Tennodai, Tsukuba
Ibaraki 305-8571 (Japan)
Fax: (+81) 29-853-4507
E-mail: nabesima@chem.tsukuba.ac.jp

[b] Dr. S. Akine, Dr. T. Nabeshima
Tsukuba Research Center for
Interdisciplinary Materials Science
University of Tsukuba, 1-1-1 Tennodai
Tsukuba, Ibaraki 305-8571 (Japan)

Supporting information for this article is available on the WWW under http://dx.doi.org/10.1002/chem.201101650.

ly bind to electron-rich aromatic compounds such as benzenediols through attractive noncovalent π–π stacking and C–H···O interactions. The parallel arrangement of the two electron-deficient aromatic terpyridine planes in **2**·4 BF_4 inspired us to utilize a similar rectangular framework for recognizing halogenated aromatic compounds on the basis of the "side-on" interaction mode between the Pt^{II}·ligand planes and the halogen atoms (Scheme 2), although the binding constants

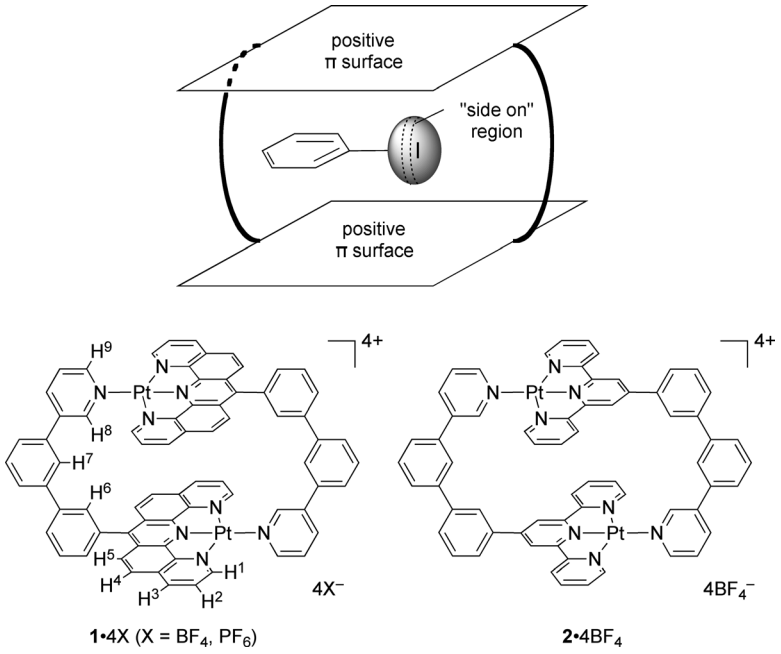

Scheme 2. Design of novel metallohosts for recognition of iodoarenes on the basis of the "side-on" interaction mode.

of **2**·4 BF_4 with chlorinated benzene derivatives were small. To enhance these noncovalent aromatic interactions, we designed and synthesized the self-assembled bis-Pt^{II} dimer **1**·4 BF_4 with extended π-face contact areas. The aromatic plane of quino[8,7-*b*][1,10]phenanthroline (dpya)[10–12] is large enough to effectively interact with a variety of benzene derivatives that bear small substituents such as halogen atoms. In addition, it has been reported that a larger aromatic π-electron surface in some metal complexes can result in a larger binding affinity to iodine substituents.[8] Thus, we envisaged that the dpya-containing metallohost $\mathbf{1}^{4+}$ would show more precise and stronger guest recognition than $\mathbf{2}^{4+}$. Gratifyingly, the host $\mathbf{1}^{4+}$ exhibited a surprisingly high binding affinity toward iodo-substituted benzene derivatives such as 1,2-diiodobenzene, 2-iodophenol, and 2,6-diiodophenol, which are substructures of the thyroid hormones T_3 and T_4.[13] This high binding affinity is considered to result from a combination of several intermolecular interactions, including "side-on" iodine···aromatic-plane and π–π stacking interactions. To the best of our knowledge, this result is the first example of an artificial receptor with high affinity toward iodinated aromatic compounds, thereby providing an important model for designing molecular recognition systems based on noncovalent iodine···aromatic-plane interactions.

Results and Discussion

Quino[8,7-*b*][1,10]phenanthroline (dpya)[10] is a tridentate chelator structurally similar to 2,2′:6′,2″-terpyridine, which has often been employed as a building unit for various metallo-supramolecular architectures[14,15] because of its strong coordination ability to metal ions. Since the aromatic plane of dpya has a more extended π-electron area than that of terpyridine, metallohosts that consist of dpya moieties would be expected to show stronger and more selective guest recognition due to various noncovalent interactions (π–π stacking, C–H···π, cation···π, and so on) for which an aromatic π-electron surface is responsible. Despite the structural similarity to terpyridine, only a few metal complexes of dpya have been reported.[11] In addition, no dpya derivative has been utilized to construct supramolecular systems to date. We predicted, however, that with its etheno bridging moiety to enhance metal-binding affinities (as seen in the differing coordination properties of 2,2′-bipyridine and 1,10-phenanthroline[16]) dpya should also exhibit strong coordination ability toward a Pt^{II} ion[17] to give the corresponding square-planar complex.

Synthesis of self-assembled bis-Pt^{II} dimer: Ligand **6** was prepared by a two-step process as outlined in Scheme 3. A palladium-catalyzed Suzuki cross-coupling reaction of **4**[12a] with the phenylboronic pinacol ester derivative **3**[9] yielded **5a**, which was partially aromatized to **5b** (detected by ESI-MS; Figure S1 in the Supporting Information). Subsequent aromatization of **5a** and **5b** produced crystalline **6**, which was characterized by a variety of analytical techniques, including NMR spectroscopy, ESI-mass spectrometry, elemental analysis, and X-ray crystallography. The single-crystal X-ray structure shows that the nitrogen atoms (N2, N4) in ligand **6** (Figure 1) are oriented in the same direction, and the dihedral angle between the plane of the terminal pyridyl ring and the plane of the central pyridyl ring of the dpya moiety is about 72°. Compound **1**·4 BF_4 was quantitatively synthesized by the reaction of the ligand **6** with $[Pt(cod)(MeCN)_2](BF_4)_2$ (cod = cyclooctadiene) prepared in situ. The ^1H NMR

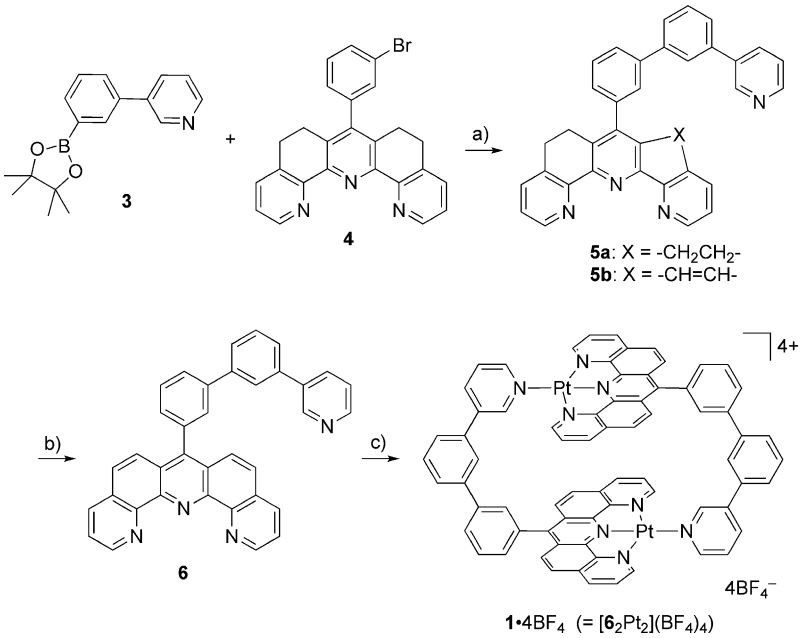

Scheme 3. Synthesis of **1**·4BF_4: a) [$Pd(PPh_3)_4$], K_2CO_3, dioxane; b) Pd/C, $C_6H_5NO_2$; c) [$Pt(cod)I_2$], $AgBF_4$, CH_3CN.

incorporates a solvent benzene molecule inside the cavity. It is noteworthy that the conformational geometry of the ligand moieties in $\mathbf{1}^{4+}$ did not significantly differ from that in the uncomplexed **6**. The angle between the ancillary pyridyl ring and the plane of the central pyridyl ring of the dpya moiety in the $\mathbf{1}^{4+}$·benzene complex remained almost unchanged (about 74°). The mean distance between the two parallel planes of the central pyridyl rings in the dpya moieties is 7.05 Å. The resultant cavity is occupied by one benzene molecule. This clearly indicates that this bis-Pt^{II} dimer $\mathbf{1}^{4+}$ is suitable for recognition of planar aromatic molecules.

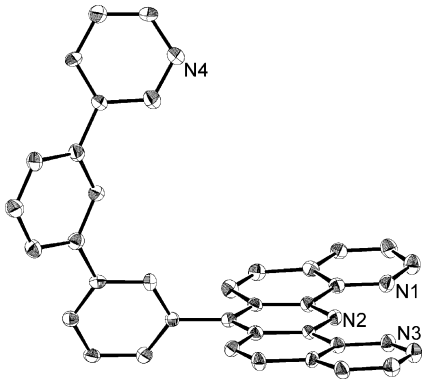

Figure 1. Crystal structure of **6** with thermal ellipsoids plotted at the 20% probability level. Hydrogen atoms are omitted for clarity.

spectrum of **1**·4BF_4 indicated the quantitative formation of one single symmetric species that showed significant downfield shifts of the pyridyl protons (H^8 and H^9; see Scheme 2 for atom numbering) due to Pt^{II} coordination and upfield shifts of the dpya protons (H1), which are probably attributable to a shielding effect by the coordinated terminal pyridyl ring (Figure S2 in the Supporting Information). Convincing evidence to support the formation of dimer $\mathbf{6}_2$·Pt^{II}_2 (=$\mathbf{1}^{4+}$) was provided by ESI-MS analysis (*m*/*z* 352.58 for $\mathbf{1}^{4+}$, 499.11 for $[\mathbf{1}+BF_4]^{3+}$, and 792.17 for $[\mathbf{1}+2BF_4]^{2+}$ (Figure S3 in the Supporting Information).

Single crystals of the metallohost suitable for X-ray crystallography were successfully obtained when the counterions were exchanged for PF_6^-. The X-ray crystallographic analysis (Figure 2) revealed a rectangular dimeric self-assembled structure that consisted of the ligand **6** and platinum(II) that

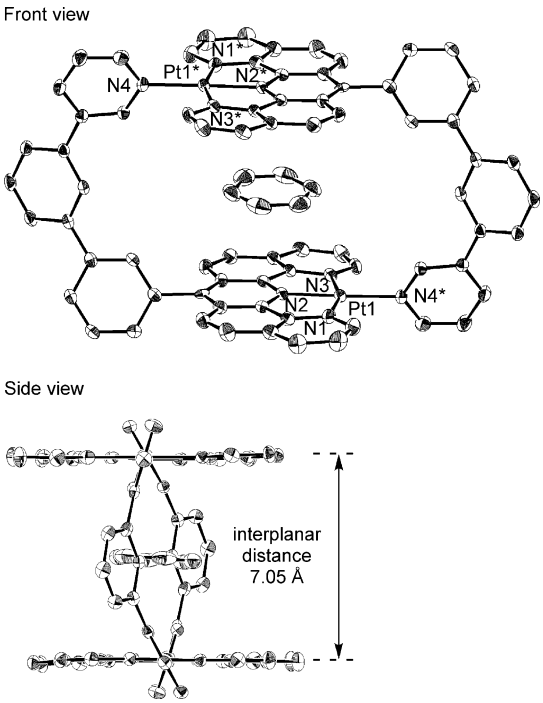

Figure 2. Crystal structure of $\mathbf{1}^{4+}$·benzene with thermal ellipsoids plotted at the 50% probability level. Solvent molecules, PF_6^- counterions, and hydrogen atoms are omitted for clarity.

Recognition of aromatic guests by $\mathbf{1}^{4+}$ and $\mathbf{2}^{4+}$: The complexation ability of $\mathbf{1}^{4+}$ with benzene derivatives in solution was studied by ^1H NMR spectroscopy. Titration experiments in [D_6]DMSO showed binding affinities of $\mathbf{1}^{4+}$ toward electron-rich benzenediols such as 1,4-benzenediol that were 8–9 times higher than those of $\mathbf{2}^{4+}$. It is particularly worth

Table 1. Association constants for various aromatic guests with **1**·4 BF_4 ($K_{a,1}$) and **2**·4 BF_4 ($K_{a,2}$).[a]

Guest	$K_{a,1}$ [M^{-1}]	$K_{a,2}$ [M^{-1}]	$K_{a,1}/K_{a,2}$
2,6-diiodophenol	35000±6000	700±20	50
1,2-diiodobenzene	21000±3000	146±10	140
2-iodophenol	16000±2000	172±3	93
1,3,5-tribromobenzene	10000±1700	102±5	98
benzene-1,4-diol	4600±300	530±30[b]	8.7
benzene-1,3-diol	3040±160	341±13[b]	8.9
1,3-diiodobenzene	2240±140	–	–
benzene-1,2-diol	2200±90	243±25[b]	9.1
1,3,5-trichlorobenzene	2100±100	–	–
1,4-dibromobenzene	1700±80	30±2	57
1,4-diiodobenzene	1650±90	81±5	20
1,3-dibromobenzene	1490±70	–	–
1,2-dibromobenzene	1240±80	27±2	46
1,4-dichlorobenzene	890±30	20±2[b]	44
1,3-dichlorobenzene	487±13	–	–
iodobenzene	403±13	–	–
1,2-dichlorobenzene	298±19	11±2[b]	27
phenol	257±10	–	–
bromobenzene	255±6	–	–
chlorobenzene	114±6	–	–
benzene	36±4	–	–
1,4-difluorobenzene	18±2	–	–

[a] Determined by ^{1}H NMR spectroscopy ([D_6]DMSO, 25°C). [b] Reported previously.[9]

noting that $\mathbf{1}^{4+}$ showed a surprisingly high binding affinity toward iodinated benzene derivatives (Table 1). The ^{1}H NMR spectra of the host $\mathbf{1}^{4+}$ upon addition of increasing amounts of 1,2-diiodobenzene are shown in Figure 3. Con-

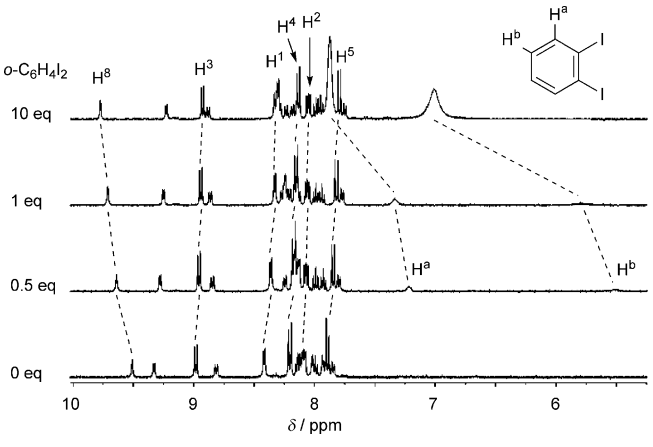

Figure 3. ^{1}H NMR spectral changes upon addition of 1,2-diiodobenzene to **1**·4 BF_4 (1 mM, [D_6]DMSO, 25°C). See Scheme 2 for proton numbering of $\mathbf{1}^{4+}$.

vincing evidence to support the formation of this host–guest complex is a large upfield shift of the 1,2-diiodobenzene protons (H^a and H^b in Figure 3). Job plots from the ^{1}H NMR spectra showed the 1:1 binding stoichiometry (Figure S4 in the Supporting Information), and the formation of the 1:1 complex was also confirmed by ESI-MS analysis (Figure S5 in the Supporting Information). In all of the titrations, the downfield shifts of the well-separated H^8 pyridyl protons have been used to determine the association constants by nonlinear least-squares regression. The K_a values of $\mathbf{1}^{4+}$ and $\mathbf{2}^{4+}$ with various guests are summarized in Table 1. It is apparent that replacement of the terpyridine units of $\mathbf{2}^{4+}$ by dpya building blocks significantly changed the recognition properties. The overall binding affinity toward planar aromatic compounds increased along with a particularly significant difference in binding affinity toward halogenated benzene derivatives. Compared to $\mathbf{2}^{4+}$, the binding affinity enhancement toward the haloarenes was at least 20-fold. A maximum enhancement of binding of 140-fold was observed with 1,2-diiodobenzene. It is noteworthy that the binding affinity tendency of $\mathbf{1}^{4+}$ and $\mathbf{2}^{4+}$ toward 1,2-diiodobenzene, 2-iodophenol, and benzene-1,2-diol is opposite. The calculated electrostatic potential surfaces (Figure S6 in the Supporting Information) of the aromatic compounds showed that there is an electronegative "side-on" region around the iodine atoms that can contribute to noncovalent interactions of the iodine atoms with the electropositive surfaces (vide infra) of dpya. From an electrostatic point of view, hydroxy-substituted benzene derivatives would form more stable complexes through π–π stacking interactions with electron-poor cationic hosts because the aromatic guests have a significantly more negative electrostatic potential surface over the aromatic ring than the haloarenes (Figure S7 in the Supporting Information). The binding tendency of $\mathbf{2}^{4+}$ is consistent with this hypothesis. However, this situation is not the case in $\mathbf{1}^{4+}$. Thus, it is reasonable to assume that strong but different noncovalent interactions between the large surface of dpya and the iodine atoms significantly contribute to the observed binding strength of $\mathbf{1}^{4+}$ toward the iodobenzene derivatives. This finding is in agreement with the results reported by Yamauchi and co-workers.[8] They suggested that the stability enhancement is caused by weak bonding interactions between the iodine atom and the pyridine ring in ternary Cu^{II} π-stacked complexes. Moreover, the electrostatic potential surfaces of chlorobenzene, bromobenzene, and iodobenzene (Figure S7)[18] show that these halobenzenes have nearly the same negative electrostatic potential over their rings. Consequently, electrostatic interactions should have a similar contribution to the guest binding. However, interactions between $\mathbf{1}^{4+}$ and monohalogenated benzenes increase when switching from chloro- to bromo-, and then to iodobenzene (K_a = 114, 255, and 403 M^{-1}, respectively). Notably, $\mathbf{1}^{4+}$ binds iodobenzene more strongly than phenol (K_a = 257 M^{-1}). This result strongly suggests the important contribution of halogen···π "side-on" interactions to the binding affinity of $\mathbf{1}^{4+}$ with the iodinated benzene derivatives. In complexes of $\mathbf{1}^{4+}$ and $\mathbf{2}^{4+}$ with disubstituted benzene derivatives, the position of the substituents of the guests also significantly affects their binding affinity. In the series of diiodobenzenes, *ortho* > *meta* > *para* selectivity was observed. The highest affinity of $\mathbf{1}^{4+}$ toward 1,2-diiodobenzene is likely the result of efficient noncovalent interactions of both of the iodine atoms with the π faces of the dpya units. The X-ray crystal structure of the complex of $\mathbf{1}^{4+}$ with 1,2-diidodobenzene

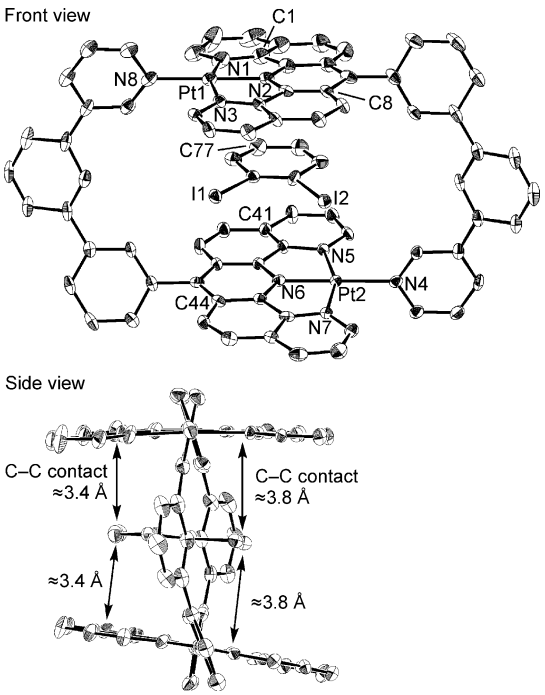

Figure 4. Crystal structure of $\mathbf{1}^{4+}$·1,2-diidodobenzene with thermal ellipsoids plotted at the 20% probability level. Solvent molecules, PF_6^- counterions, and hydrogen atoms are omitted for clarity.

(Figure 4) clearly shows that 1,2-diiodobenzene is deeply buried inside the cavity. Both of the iodine atoms make van der Waals contacts with carbon atoms of the dpya units with the shortest interatomic C···I contact near 3.8 Å (C44–I1, C8–I2). In addition, π–π stacking interactions were found between the host and guest aromatic rings with the shortest interatomic contact at about 3.4 Å (C77–C1, C77–C41). Thus, the two dpya units of $\mathbf{1}^{4+}$ are no longer parallel to each other and give a slightly tilted structure; the iodine side of $\mathbf{1}^{4+}$ is more widely open to accommodate the two iodine atoms. The electrostatic potential surface was determined by using theoretical calculations based on the X-ray host structure to confirm that the inner dpya walls provide a positively charged binding cavity (Figure 5). Interestingly, the surface of the inner walls is more positive than that of the outside as seen in $\mathbf{2}^{4+}$. This result again supports the hypothesis that the cavity should be suitable for arene recognition. Excellent similarity between the solution and solid-state structures of the $\mathbf{1}^{4+}$·1,2-diiodobenzene complex was supported by NOESY measurements, in which NOE correlations were observed between the inner cavity protons (H^6, H^7, and H^8) of $\mathbf{1}^{4+}$ and the H^a protons of 1,2-diiodobenzene (Scheme 4). Additionally, the H^b protons of 1,2-diiodobenzene exhibited a larger upfield shift ($\Delta\delta \approx 1.84$; Figure 6) than the H^a protons ($\Delta\delta \approx 0.83$). The single-crystal X-ray diffraction structure of the $\mathbf{1}^{4+}$·1,2-diiodobenzene complex thoroughly elucidates the larger upfield shift, because in the solid the H^b protons are located at the position that is most affected by the anisotropic effect of the dpya planes.

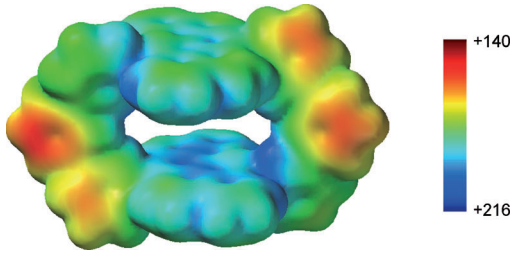

Figure 5. Electrostatic potential surface of $\mathbf{1}^{4+}$ calculated by DFT (B3LYP, 6-31G*, single-point calculation[19]) with the crystal structure of $\mathbf{1}^{4+}$ as input.

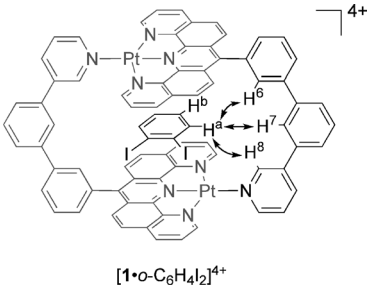

Scheme 4. Illustration of observed intermolecular NOE correlations between $\mathbf{1}^{4+}$ and 1,2-diiodobenzene.

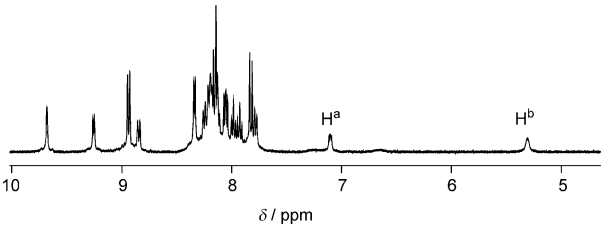

Figure 6. ^{1}H NMR spectrum of a mixture of $\mathbf{1}$·4 BF_4 and 1,2-diiodobenzene ([$\mathbf{1}$·4 BF_4] = 6 mM, [1,2-diiodobenzene] = 3 mM, [D_6]DMSO, 25 °C), >98% of the guest in bound form.

Interestingly, compared to its selectivity for diiodobenzenes, the selectivity of $\mathbf{1}^{4+}$ toward benzenediols, dichlorobenzenes, and dibromobenzenes was reversed, and a *para* > *meta* > *ortho* trend was observed. This selectivity strongly suggests that additional noncovalent interactions with inside cavity protons such as C–H···O, C–H···Cl, and C–H···Br influence the binding of benzenediols, dichlorobenzenes, and dibromobenzenes by $\mathbf{1}^{4+}$. Interestingly, the *para* > *meta* > *ortho* trend is more significant in the series of dichlorobenzenes than with dibromobenzenes. This fact may suggest that the larger bonding strength of C–H···halogen interactions more effectively determines the binding selectivity. The *para* > *meta* > *ortho* binding selectivity trend of $\mathbf{1}^{4+}$ toward benzenediols was also observed for the terpyridine-based dimer $\mathbf{2}^{4+}$, which we have previously reported.[9] We found that the protons of $\mathbf{2}^{4+}$ inside the cavity form multiple

C–H···O hydrogen bonds with the oxygen atoms of guest benzenediol molecules. It is therefore reasonable to assume that C–H···O hydrogen bonding also controls the binding of benzenediols by $\mathbf{1}^{4+}$. X-ray crystallographic analysis clearly rationalized the selectivity of $\mathbf{1}^{4+}$ toward benzene-1,4-diol (Figure 7a). In the crystal structure, the guest benzene-1,4-diol is held inside the cavity between the two platinum-containing aromatic planes. The mean distance between the two parallel planes of the central pyridyl rings in the dpya moieties is 6.72 Å, indicative of the efficient π–π stacking interactions between $\mathbf{1}^{4+}$ and benzene-1,4-diol. In addition to the parallel-displaced π–π stacking interactions, there are significant C–H···O hydrogen bonds between the sidewall protons of the cavity of $\mathbf{1}^{4+}$ and the hydroxy oxygen atoms of benzene-1,4-diol. For example, the shortest C···O distance is 3.434(11) Å (C21–O1*; the H···O distance is 2.55 Å and the C–H···O angle is 155.14°). The centrosymmetric crystal structure of $\mathbf{1}^{4+}$·benzene-1,4-diol clearly indicates that both hydroxy groups of benzene-1,4-diol can simultaneously interact with the host sidewall with the C–H···O interaction. On the other hand, only one of the hydroxy groups of benzene-1,3- and -1,2-diols can participate in the C–H···O interaction because of the shorter OH–OH distances (Figure 7b and c). This difference may account for the selectivity of $\mathbf{1}^{4+}$ toward benzene-1,4-diol among the three isomers. It should also be noted that the highest association constant among the investigated guests was observed for 2,6-diiodophenol. The association constant of $35000\,\mathrm{M}^{-1}$ is much higher than those of the three diiodobenzenes ($1650–21000\,\mathrm{M}^{-1}$) or 2-iodophenol ($16000\,\mathrm{M}^{-1}$). This result clearly indicates that both of the halogen atoms and the hydroxy group contribute to the strong binding. The X-ray structure also confirmed that 2,6-diiodophenol is suitably sandwiched between the two dpya moieties of $\mathbf{1}^{4+}$ (Figure 8). It is well known that the 2,6-diiodophenyl fragment is seen in thyroid hormones such as thyroxin and triiodothyronine as well as their precursor, diiodotyrosine. The platinum-containing framework of $\mathbf{1}^{4+}$ that bears cationic, large π-aromatic surfaces should therefore be potentially useful as the binding part of a receptor that can selectively bind such thyroid hormone derivatives.

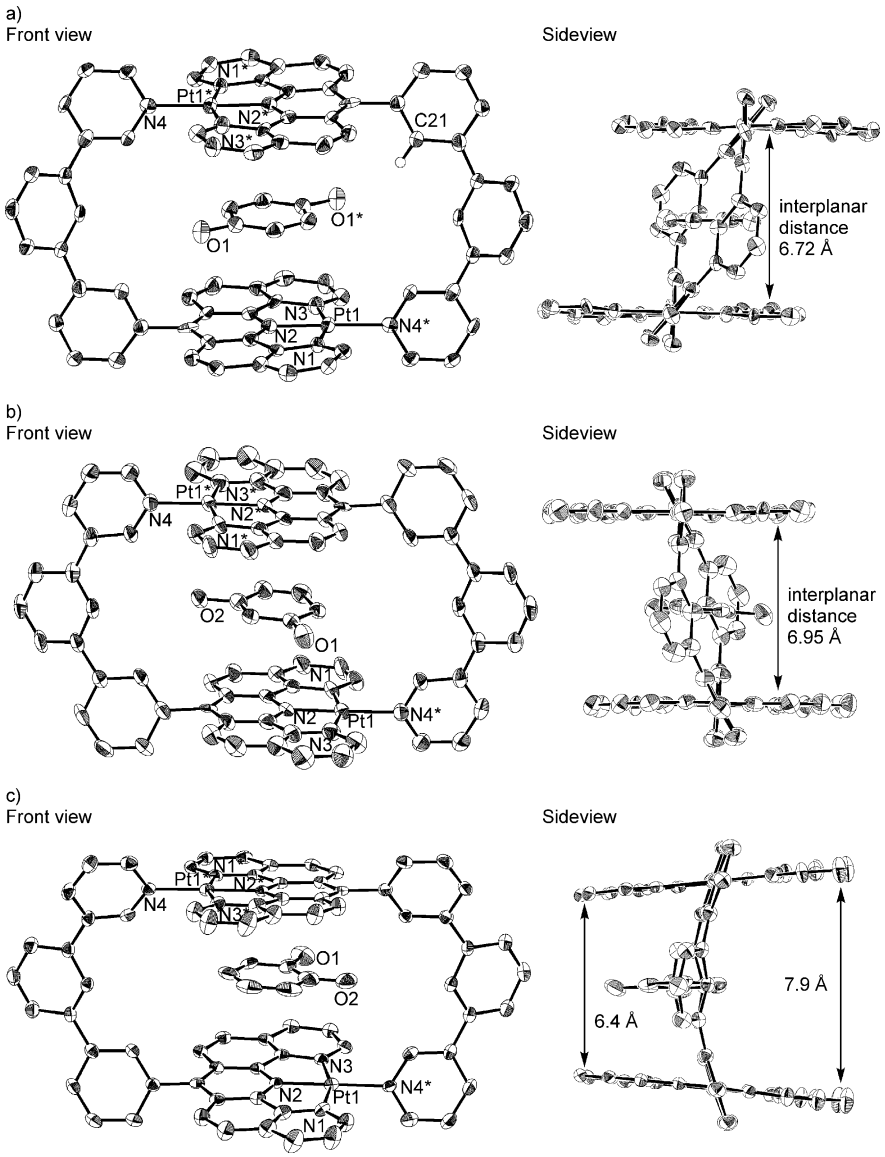

Figure 7. Crystal structures of a) $\mathbf{1}^{4+}$·benzene-1,4-diol, b) $\mathbf{1}^{4+}$·benzene-1,3-diol, and c) $\mathbf{1}^{4+}$·benzene-1,2-diol with thermal ellipsoids plotted at the 50% probability level. Solvent molecules, counterions, and hydrogen atoms are omitted for clarity.

Conclusion

Coordination of **6** to Pt^{II} quantitatively gave the macrocyclic metallodimer $\mathbf{1}^{4+}$, which showed efficient recognition of planar aromatic guest molecules as evidenced by ^{1}H NMR spectroscopy and X-ray diffraction studies. The metalloreceptor $\mathbf{1}^{4+}$ was designed on the basis of rational derivatization of previously reported $\mathbf{2}^{4+}$ through the extension of the π-recognition area. Despite their structural similarity, a dramatic change in selectivity toward substituted benzene derivatives was observed for $\mathbf{1}^{4+}$ compared to $\mathbf{2}^{4+}$. ^{1}H NMR spectroscopic

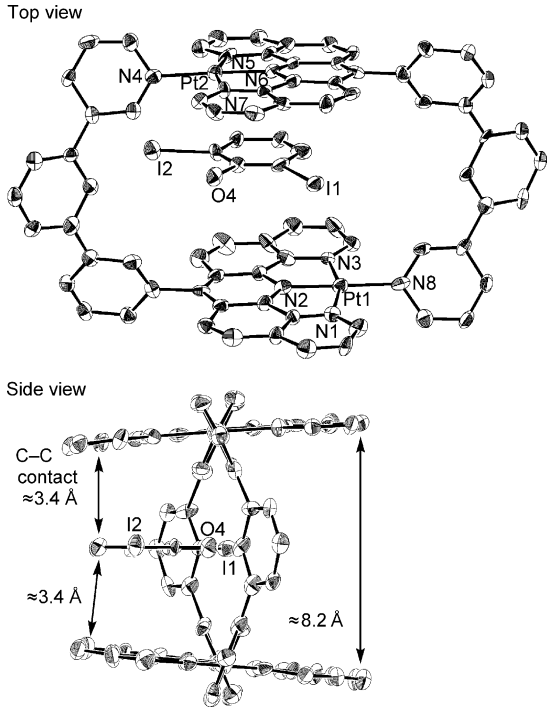

Figure 8. Crystal structure of $\mathbf{1}^{4+}$·2,6-diiodophenol with thermal ellipsoids plotted at the 20% probability level. Solvent molecules, PF_6^- counterions, and hydrogen atoms are omitted for clarity.

titration revealed a high affinity of $\mathbf{1}^{4+}$ towards haloarenes, with exceptionally large association constants for 2-iodophenol ($K_a = 16000\,M^{-1}$) and 1,2-diiodobenzene ($K_a = 21000\,M^{-1}$), which are 93- and 140-fold higher, respectively, than the values obtained for $\mathbf{2}^{4+}$. In addition, $\mathbf{1}^{4+}$ showed a remarkably high affinity and selectivity toward 2,6-diiodophenol ($K_a = 35000\,M^{-1}$), which is an important substructure of the thyroid hormone T_4. Structural analyses strongly suggest that "side-on" iodine···aromatic plane interactions and π–π stacking contribute to the strong 1,2-diiodobenzene and 2,6-diiodophenol binding. The results obtained here give unique and valuable insight into the nature of halogen atom interactions in their "side-on" region with an electropositive aromatic plane, which may provide useful guidance for designing artificial receptors for iodinated biomolecules.

Experimental Section

General: All of the chemicals were of reagent grade and were used as received. The NMR spectroscopic experiments were performed using a Bruker AVANCE400 spectrometer. [D_6]DMSO was used in all the NMR spectroscopic titration measurements as the solvent of choice due to the low solubility of $\mathbf{1}$·4BF_4 in other common solvents. The chemical shifts were measured from the internal TMS reference. All the NMR spectroscopic data were processed using the iNMR software (version 2.3.1). Mass spectra under the conditions of electrospray ionization were recorded using an Applied Biosystems Qstar/Pulsar *i*. Elemental analyses were performed using a Yanagimoto CHN corder MT-6. Melting points were obtained using a Yanaco melting-point apparatus and are uncorrected. 2,6-Diiodophenol was synthesized according to the literature.[20]

Synthesis of compound 5a: Compound **4**[12a] (6.69 g, 15.2 mmol), **3**[9] (4.96 g, 17.6 mmol), and tetrakis(triphenylphosphane)palladium(0) (0.88 g, 0.76 mmol) were placed in a 250 mL round-bottomed flask. Dioxane (100 mL) degassed through three freeze–pump–thaw cycles and potassium carbonate (5.25 g, 38.0 mmol) was added, and the resulting mixture was then stirred at 80 °C for 16 h. The mixture was poured into water and extracted with chloroform (80 mL four times). The combined organic layer was dried over anhydrous magnesium sulfate. The solvents were removed and the crude product was purified by column chromatography ($CHCl_3$/MeOH/Et_3N 50:6:1) to give a mixture of **5a** and **5b** (6.2 g, about 80%), which was used in the next step without further purification.

Synthesis of compound 6: The mixture of **5a** and **5b** (1.84 g, about 3.6 mmol), 10% Pd/C (1.37 g), and nitrobenzene (110 mL) were placed together into a 250 mL round-bottomed flask. The resulting mixture was then stirred at 150 °C under argon for 3.5 h. The reaction mixture was then cooled, the catalyst was filtered through a celite bed, and the filter cake was washed with methanol and dichloromethane. Solvents were removed under reduced pressure and the residue was subjected to column chromatography ($CHCl_3$/MeOH/NH_{3aq} 50:6:0.03) on silica gel to afford **6** (1.24 g, 2.43 mmol, 68%) as a white solid. M.p. ≥300 °C; ^{1}H NMR (400 MHz, [D_6]DMSO): $\delta = 7.46$ (dd, $J = 7.9$, 4.8 Hz, 1H), 7.61 (d, $J = 7.1$ Hz, 1H), 7.64 (t, $J = 7.6$ Hz, 1H), 7.72 (d, $J = 9.2$ Hz, 2H), 7.76 (d, $J = 7.6$ Hz, 1H), 7.86 (t, $J = 7.8$ Hz, 1H), 7.89–7.92 (m, 3H), 8.01 (d, $J = 9.2$ Hz, 2H), 8.11 (s, 1H), 8.14 (s, 1H), 8.14–8.19 (m, 2H), 8.55–8.57 (m, 3H), 9.00 (d, $J = 2.1$ Hz, 1H), 9.27 ppm (d, $J = 3.2$ Hz, 2H); ^{13}C NMR (100 MHz, $CDCl_3$): $\delta = 123.61$, 123.78, 125.07, 126.18, 126.32, 126.66, 126.92, 127.04, 127.40, 128.84, 129.19, 129.38, 129.77, 134.52, 136.13, 136.42, 136.62, 138.73, 141.22, 141.25, 145.81, 146.41, 146.85, 148.39, 148.75, 150.15 ppm; ESI-MS (positive): m/z: 511 $[M+H]^+$; elemental analysis calcd (%) for $C_{36}H_{22}N_4$·1.3H_2O: C 80.97, H 4.64, N 10.49; found: C 80.87, H 4.63, N 10.12.

Synthesis of bis(μ-{7-[3′-(3-pyridinyl-κ*N*)(1,1′-biphenyl)-3-yl]quino[8,7-*b*]-[1,10]phenanthroline-κN^1,κ$N^{1'}$,κ$N^{1''}$})diplatinum(4+) tetrafluoroborate (1·4BF_4): Silver tetrafluoroborate (168 mg, 0.863 mmol) was added to a suspension of (cycloocta-1,5-diene)diiodoplatinum(II) (230 mg, 0.413 mmol) in acetone (5 mL), and the mixture was stirred for 10 min. Then the AgI precipitate was removed by filtration, and the solvent was evaporated. The obtained residue was dissolved in acetonitrile (10 mL) and then added to a solution of **6** (109 mg, 0.213 mmol) in acetonitrile (70 mL). The reaction mixture was stirred at room temperature for 3 days. The solvents were evaporated to dryness, and the residue was treated with acetone. The yellow solid was filtered off, washed with water, then acetone, and dried in vacuum to afford **1**·4BF_4 (185 mg, 0.0918 mmol, 86%). ^{1}H NMR (400 MHz, [D_6]DMSO): $\delta = 7.84$ (d, $J = 7.6$ Hz, 2H), 7.89 (d, $J = 9.4$ Hz, 4H), 7.90 (t, $J = 7.9$ Hz, 2H), 7.94 (s, 2H), 7.99 (t, $J = 7.6$ Hz, 2H), 8.03 (s, 2H), 8.08 (dd, $J = 8.2$, 5.3 Hz, 4H), 8.08 (d, $J = 7.9$ Hz, 2H), 8.13 ($J = 7.9$ Hz, 2H), 8.13 (dd, $J = 8.4$, 5.1 Hz, 2H), 8.20 (d, $J = 9.4$ Hz, 4H), 8.20 (d, $J = 7.6$ Hz, 2H), 8.41 (d, $J = 5.3$ Hz, 4H), 8.81 (dt, $J = 8.4$, 1.5 Hz, 2H), 8.98 (d, $J = 8.1$ Hz, 4H), 9.33 (d, $J = 5.1$ Hz, 2H), 9.52 ppm (d, $J = 1.3$ Hz, 2H); ^{13}C NMR (100 MHz, [D_6]DMSO): $\delta = 126.21$, 126.55, 127.19, 127.42, 128.22, 128.48, 128.86, 129.09, 129.35, 129.43, 129.56, 130.36, 130.70, 132.18, 132.51, 135.48, 139.14, 139.51, 140.11, 140.73, 141.64, 144.43, 149.89, 151.04, 151.48, 154.36 ppm; ESI-MS (positive): m/z: 352.58 [$\mathbf{1}^{4+}$]; elemental analysis calcd (%) for $C_{72}H_{44}B_4F_{16}N_8Pt_2$·$CH_3CN$·1.8$CHCl_3$: C 45.19, H 2.44, N 6.26; found: C 45.19, H 2.65, N 6.40.

^{1}H NMR spectroscopic titration: For each complex, 11 samples were prepared with an increasing guest/host ratio. For each one, a stock solution (250 μL) of host (4 mM) was mixed with a varying amount of a stock solution of guest, and the volume was adjusted to 500 μL. All ^{1}H NMR spectroscopic titration measurements were performed at least twice and were carried out at 25 °C (controlled by the temperature-control system of the NMR spectrometer).

X-ray structure determination: Single crystals of **6** suitable for X-ray crystallography were obtained by the slow diffusion of diethyl ether into a solution of **6** in dichloromethane. Single crystals of **1**·4PF_6·benzene complex were obtained by the slow diffusion of benzene into a solution

of **1**·4 BF_4 in DMSO that contained 50 equiv of $nBu_4N{\cdot}PF_6$. Single crystals of the host–guest complexes of $\mathbf{1}^{4+}$ were obtained by the slow diffusion of benzene into a mixture of **1**·4 BF_4, guest, and 50 equiv of $nBu_4N{\cdot}PF_6$ in DMSO. The X-ray diffraction intensities were collected with $Mo_{K\alpha}$ radiation ($\lambda = 0.71069$ Å) at 120 K by using a Rigaku R-AXIS RAPID diffractometer. The reflection data were corrected for Lorentz and polarization factors, and for absorption using the multiscan method. The structure was solved by Patterson methods (DIRDIF 99[21]) and refined by full-matrix least-squares on F^2 by using all the data (SHELXL 97[22]). The crystallographic data are summarized in Tables 2, 3, and 4.

Table 2. Crystallographic data.

Compound	**6**	**1**·4 PF_6·4 DMSO·5 C_6H_6	**1**·4 PF_6·1,2-$C_6H_4I_2$·1.4 DMSO·6.6 C_6H_6
formula	$C_{36}H_{22}N_4$	$C_{110}H_{98}F_{24}N_8O_4P_4Pt_2S_4$	$C_{120.4}H_{96}F_{24}I_2N_8O_{1.4}P_4Pt_2S_{1.4}$
M_r	510.58	2694.26	2946.00
crystal system	monoclinic	triclinic	triclinic
space group	$P2_1/n$	$P\bar{1}$	$P\bar{1}$
a [Å]	10.23(2)	13.3367(5)	13.9884(13)
b [Å]	25.32(4)	14.1431(4)	14.1274(14)
c [Å]	10.235(16)	15.6832(5)	29.345(2)
α [°]	90.00	89.3924(9)	90.088(2)
β [°]	108.40(6)	73.2174(11)	92.782(2)
γ [°]	90.00	72.0142(11)	105.682(3)
V [Å^3]	2515(7)	2683.76(15)	5576.1(9)
Z	4	1	2
T [K]	120	120	120
ρ_{calcd} [g cm^{-3}]	1.348	1.667	1.755
R_1[a] ($I > 2\sigma(I)$)	0.0613	0.0367	0.0871
wR_2[a] (all data)	0.1131	0.0906	0.2497

[a] $R_1 = \Sigma||F_o|-|F_c||/\Sigma|F_o|$; $wR_2 = \{\Sigma[w(F_o^2-F_c^2)^2]/\Sigma[w(F_o^2)^2]\}^{1/2}$.

Table 3. Crystallographic data (continued).

Compound	**1**·2 PF_6·2 BF_4·1,2-$C_6H_4[OH]_2$·8 DMSO·2 C_6H_6	**1**·4 PF_6·1,3-$C_6H_4[OH]_2$·6 DMSO·3 C_6H_6
formula	$C_{106}H_{110}B_2F_{20}N_8O_{10}P_2Pt_2S_8$	$C_{108}H_{104}F_{24}N_8O_8P_4Pt_2S_6$
M_r	2766.24	2804.41
crystal system	monoclinic	triclinic
space group	$C2/c$	$P\bar{1}$
a [Å]	33.767(2)	13.4345(9)
b [Å]	15.5570(10)	14.1445(8)
c [Å]	25.7970(15)	15.7840(8)
α [°]	90.00	92.7808(16)
β [°]	116.7028(14)	108.4957(17)
γ [°]	90.00	104.8879(19)
V [Å^3]	12106.4(13)	2721.1(3)
Z	4	1
T [K]	120	120
ρ_{calcd} [g cm^{-3}]	1.518	1.711
R_1[a] ($I > 2\sigma(I)$)	0.0687	0.0695
wR_2[a] (all data)	0.2117	0.2133

[a] $R_1 = \Sigma||F_o|-|F_c||/\Sigma|F_o|$; $wR_2 = \{\Sigma[w(F_o^2-F_c^2)^2]/\Sigma[w(F_o^2)^2]\}^{1/2}$.

CCDC-827322 (**1**·4 PF_6·4 DMSO·5 C_6H_6), CCDC-827323 (**1**·2 PF_6·2 BF_4·1,2-$C_6H_4(OH)_2$·8 DMSO·2 C_6H_6), CCDC-827324 (**1**·4 PF_6·1,2-$C_6H_4I_2$·1.4 DMSO·6.6 C_6H_6), CCDC-827325 (**1**·4 PF_6·2.33 $C_6H_3I_2OH$·0.33 C_6H_6·2 DMSO), CCDC-827326 (**1**·4 PF_6·1,4-$C_6H_4(OH)_2$·4 DMSO·5 C_6H_6), CCDC-827327 (**1**·4 PF_6·1,3-$C_6H_4(OH)_2$·6 DMSO·3 C_6H_6), and CCDC-827328 (**6**) contain the supplementary crystallographic data for this paper. These data can be obtained free of charge from The Cambridge Crystallographic Data Centre via www.ccdc.cam.ac.uk/data_request/cif.

Table 4. Crystallographic data (continued).

Compound	**1**·4 PF_6·1,4-$C_6H_4[OH]_2$·4 DMSO·5 C_6H_6	**1**·4 PF_6·2.33 $C_6H_3I_2OH$·2 DMSO·0.33 C_6H_6
formula	$C_{116}H_{104}F_{24}N_8O_6P_4Pt_2S_4$	$C_{92}H_{67.33}F_{24}I_{4.67}N_8O_{4.33}P_4Pt_2S_2$
M_r	2804.37	2980.59
crystal system	triclinic	monoclinic
space group	$P\bar{1}$	$C2/c$
a [Å]	11.8059(8)	65.719(5)
b [Å]	14.7076(9)	14.7112(13)
c [Å]	16.8096(13)	30.962(2)
α [°]	98.035(2)	90.00
β [°]	106.941(2)	96.7679(16)
γ [°]	91.0846(18)	90.00
V [Å^3]	2759.2(3)	29726(4)
Z	1	12
T [K]	120	120
ρ_{calcd} [g cm^{-3}]	1.688	1.998
R_1[a] ($I > 2\sigma(I)$)	0.0641	0.1166
wR_2[a] (all data)	0.1765	0.3144

[a] $R_1 = \Sigma||F_o|-|F_c||/\Sigma|F_o|$; $wR_2 = \{\Sigma[w(F_o^2-F_c^2)^2]/\Sigma[w(F_o^2)^2]\}^{1/2}$.

Acknowledgements

This work was supported by Grants-in-Aid for Scientific Research from the Ministry of Education, Culture, Sports, Science and Technology, Japan.

[1] For reviews, see: a) P. Metrangolo, G. Resnati, *Chem. Eur. J.* **2001**, *7*, 2511–2519; b) P. Metrangolo, H. Neukirch, T. Pilati, G. Resnati, *Acc. Chem. Res.* **2005**, *38*, 386–395; c) P. Politzer, P. Lane, M. C. Concha, Y. Ma, J. S. Murray, *J. Mol. Model.* **2007**, *13*, 305–311; d) *Halogen Bonding: Fundamentals and Applications* (Eds.: P. Metrangolo, G. Resnati), Springer, Berlin, **2008**; e) P. Metrangolo, G. Resnati, *Science* **2008**, *321*, 918–919.

[2] a) J. P. M. Lommerse, A. J. Stone, R. Taylor, F. H. Allen, *J. Am. Chem. Soc.* **1996**, *118*, 3108–3116; b) P. Metrangolo, F. Meyer, T. Pilati, G. Resnati, G. Terraneo, *Angew. Chem.* **2008**, *120*, 6206–6220; *Angew. Chem. Int. Ed.* **2008**, *47*, 6114–6127; c) R. Bertani, P. Sgarbossa, A. Venzo, F. Lelj, M. Amati, G. Resnati, T. Pilati, P. Metrangolo, G. Terraneo, *Coord. Chem. Rev.* **2010**, *254*, 677–695; d) G. Cavallo, P. Metrangolo, T. Pilati, G. Resnati, M. Sansotera, G. Terraneo, *Chem. Soc. Rev.* **2010**, *39*, 3772–3783.

[3] a) P. Auffinger, F. A. Hays, E. Westhof, P. S. Ho, *Proc. Natl. Acad. Sci. USA* **2004**, *101*, 16789–16794; b) A. R. Voth, F. A. Hays, P. S. Ho, *Proc. Natl. Acad. Sci. USA* **2007**, *104*, 6188–6193; c) A. R. Voth, P. Khuu, K. Oishi, P. S. Ho, *Nat. Chem.* **2009**, *1*, 74–79; d) Y. Lu, T. Shi, Y. Wang, H. Yang, X. Yan, X. Luo, H. Jiang, W. Zhu, *J. Med. Chem.* **2009**, *52*, 2854–2862; e) P. Metrangolo, G. Resnati, *Nat. Chem.* **2011**, *3*, 260.

[4] a) L. Brammer, E. A. Bruton, P. Sherwood, *Cryst. Growth Des.* **2001**, *1*, 277–290; b) Y. Lu, Y. Wang, Z. Xu, X. Yan, X. Luo, H. Jiang, W. Zhu, *J. Phys. Chem. B* **2009**, *113*, 12615–12621.

[5] For a review, see: R. J. Kulawiec, R. H. Crabtree, *Coord. Chem. Rev.* **1990**, *99*, 89–115.

[6] For iodoarenes as ligands for transition metals, see: a) R. H. Crabtree, J. W. Faller, M. F. Mellea, J. M. Quirk, *Organometallics* **1982**, *1*, 1361–1366; b) C. H. Winter, W. R. Veal, C. M. Garner, A. M. Arif, J. A. Gladysz, *J. Am. Chem. Soc.* **1989**, *111*, 4766–4776; c) R. J. Ku-

lawiec, J. W. Faller, R. H. Crabtree, *Organometallics* **1990**, *9*, 745–755; d) T. M. Gomes-Carneiro, R. D. Jackson, J. H. Downing, A. G. Orpen, P. G. Pringle, *J. Chem. Soc. Chem. Commun.* **1991**, 317–319; e) J. Powell, M. Horvath, A. Lough, *J. Chem. Soc. Chem. Commun.* **1993**, 733–735; f) J. Powell, M. J. Horvath, A. Lough, *J. Chem. Soc. Dalton Trans.* **1996**, 1669–1677; g) M. D. Butts, B. L. Scott, G. J. Kubas, *J. Am. Chem. Soc.* **1996**, *118*, 11831–11843; h) H. N. Aliyu, R. D. Gillard, J. D. Honeywill, P. Lightfoot, J. Rocha, *Polyhedron* **1996**, *15*, 2409–2419; i) P. J. Albietz, Jr. B. P. Cleary, W. Paw, R. Eisenberg, *J. Am. Chem. Soc.* **2001**, *123*, 12091–12092.

[7] T. Clark, M. Hennemann, J. S. Murray, P. Politzer, *J. Mol. Model.* **2007**, *13*, 291–296.

[8] a) T. Sugimori, H. Masuda, O. Yamauchi, *Bull. Chem. Soc. Jpn.* **1994**, *67*, 131–137; b) F. Zhang, A. Odani, H. Masuda, O. Yamauchi, *Inorg. Chem.* **1996**, *35*, 7148–7155; c) F. Zhang, T. Yajima, H. Masuda, A. Odani, O. Yamauchi, *Inorg. Chem.* **1997**, *36*, 5777–5784.

[9] a) R. Trokowski, S. Akine, T. Nabeshima, *Chem. Commun.* **2008**, 889–890; b) R. Trokowski, S. Akine, T. Nabeshima, *Dalton Trans.* **2009**, 10359–10366.

[10] a) E. Koft, F. H. Case, *J. Org. Chem.* **1962**, *27*, 865–868; b) T. R. Kelly, R. L. Lebedev, *J. Org. Chem.* **2002**, *67*, 2197–2205.

[11] a) C.-Y. Hung, T.-L. Wang, Y. Jang, W. Y. Kim, R. H. Schmehl, R. P. Thummel, *Inorg. Chem.* **1996**, *35*, 5953–5956; b) J. H. Groen, A. de Zwart, M. J. M. Vlaar, J. M. Ernsting, P. W. N. M. van Leeuwen, K. Vrieze, H. Kooijman, W. J. J. Smeets, A. L. Spek, P. H. M. Budzelaar, Q. Xiang, R. P. Thummel, *Eur. J. Inorg. Chem.* **1998**, 1129–1143; c) H. Chen, R. Tagore, S. Das, C. Incarvito, J. W. Faller, R. H. Crabtree, G. W. Brudvig, *Inorg. Chem.* **2005**, *44*, 7661–7670; d) C. Duboc, V. Astier-Perret, H. Chen, J. Pécaut, R. H. Crabtree, G. W. Brudvig, M.-N. Collomb, *Inorg. Chim. Acta* **2006**, *359*, 1541–1548; e) G. D. Jones, J. L. Martin, C. McFarland, O. R. Allen, R. E. Hall, A. D. Haley, R. J. Brandon, T. Konovalova, P. J. Desrochers, P. Pulay, D. A. Vicic, *J. Am. Chem. Soc.* **2006**, *128*, 13175–13183; f) S. Zein, C. Duboc, W. Lubitz, F. Neese, *Inorg. Chem.* **2008**, *47*, 134–142; g) S. Zein, F. Neese, *J. Phys. Chem. A* **2008**, *112*, 7976–7983.

[12] For related "U-shaped" terpyridine ligands and their complexes, see: a) D. Sielemann, A. Winter, U. Flörke, N. Risch, *Org. Biomol. Chem.* **2004**, *2*, 863–868; b) A. Winter, J. Hummel, N. Risch, *J. Org. Chem.* **2006**, *71*, 4862–4871; c) K. Sénéchal-David, A. Hemeryck, N. Tancrez, L. Toupet, J. A. G. Williams, I. Ledoux, J. Zyss, A. Boucekkine, J.-P. Guégan, H. Le Bozec, O. Maury, *J. Am. Chem. Soc.* **2006**, *128*, 12243–12255.

[13] a) R. L. Wagner, J. W. Apriletti, M. E. McGrath, B. L. West, J. D. Baxter, R. J. Fletterick, *Nature* **1995**, *378*, 690–697; b) M. Gurnell, O. Rajanayagam, M. Agostini, R. J. D. Clifton-Bligh, T. Wang, P. M. J. Zelissen, F. van der Horst, A. van de Wiel, E. Macchia, A. Pinchera, J. W. R. Schwabe, V. K. K. Chatterjee, *Endocrinology* **1999**, *140*, 5901–5906; c) A. Wojtczak, V. Cody, J. R. Luft, W. Pangborn, *Acta Crystallogr. Sect. D* **2001**, *57*, 1061–1070; d) B. Sandler, P. Webb, J. W. Apriletti, B. R. Huber, M. Togashi, S. T. Cunha Lima, S. Juric, S. Nilsson, R. Wagner, R. J. Fletterick, J. D. Baxter, *J. Biol. Chem.* **2004**, *279*, 55801–55808.

[14] For reviews on terpyridine-containing supramolecules, see: a) A. M. W. Cargill Thompson, *Coord. Chem. Rev.* **1997**, *160*, 1–52; b) H. Hofmeier, U. S. Schubert, *Chem. Soc. Rev.* **2004**, *33*, 373–399; c) I. Eryazici, C. N. Moorefield, G. R. Newkome, *Chem. Rev.* **2008**, *108*, 1834–1895; d) E. C. Constable, *Coord. Chem. Rev.* **2008**, *252*, 842–855.

[15] For terpyridine-containing cleft hosts, see: a) R. D. Sommer, A. L. Rheingold, A. J. Goshe, B. Bosnich, *J. Am. Chem. Soc.* **2001**, *123*, 3940–3952; b) A. J. Goshe, J. D. Crowley, B. Bosnich, *Helv. Chim. Acta* **2001**, *84*, 2971–2985; c) A. J. Goshe, I. M. Steele, C. Ceccarelli, A. L. Rheingold, B. Bosnich, *Proc. Natl. Acad. Sci. USA* **2002**, *99*, 4823–4829; d) A. J. Goshe, I. M. Steele, B. Bosnich, *J. Am. Chem. Soc.* **2003**, *125*, 444–451; e) J. D. Crowley, A. J. Goshe, B. Bosnich, *Chem. Commun.* **2003**, 392–393; f) J. D. Crowley, A. J. Goshe, B. Bosnich, *Chem. Commun.* **2003**, 2824–2825; g) J. D. Crowley, A. J. Goshe, I. M. Steele, B. Bosnich, *Chem. Eur. J.* **2004**, *10*, 1944–1955; h) A. J. Goshe, I. M. Steele, B. Bosnich, *Inorg. Chim. Acta* **2004**, *357*, 4544–4551; i) J. D. Crowley, I. M. Steele, B. Bosnich, *Eur. J. Inorg. Chem.* **2005**, 3907–3917; j) J. D. Crowley, B. Bosnich, *Eur. J. Inorg. Chem.* **2005**, 2015–2025; k) J. D. Crowley, I. M. Steele, B. Bosnich, *Inorg. Chem.* **2005**, *44*, 2989–2991.

[16] a) K. Yamasaki, M. Yasuda, *J. Am. Chem. Soc.* **1956**, *78*, 1324; b) R. H. Holyer, C. D. Hubbard, S. F. A. Kettle, R. G. Wilkins, *Inorg. Chem.* **1965**, *4*, 929–935.

[17] For reviews on platinum-based supramolecules, see: a) M. Fujita, K. Umemoto, M. Yoshizawa, N. Fujita, T. Kusukawa, K. Biradha, *Chem. Commun.* **2001**, 509–518; b) P. H. Dinolfo, J. T. Hupp, *Chem. Mater.* **2001**, *13*, 3113–3125; c) B. H. Northrop, Y.-R. Zheng, K.-W. Chi, P. J. Stang, *Acc. Chem. Res.* **2009**, *42*, 1554–1563.

[18] N. Hallowita, E. Udonkang, C. Ruan, C. E. Frieler, M. T. Rodgers, *Int. J. Mass Spectrom.* **2009**, *283*, 35–47.

[19] *Spartan '04*, Wavefunction, Irvine, CA, **2004**.

[20] M. Jereb, M. Zupan, S. Stavber, *Chem. Commun.* **2004**, 2614–2615.

[21] P. T. Beurskens, G. Beurskens, R. de Gelder, S. Garcia-Granda, R. O. Gould, R. Israel, J. M. M. Smits, *The DIRDIF-99 Program system*, Crystallography Laboratory, University of Nijmegen, Nijmegen, The Netherlands, **1999**.

[22] SHELXL 97, program for crystal structure refinement: G. M. Sheldrick, *Acta Crystallograph. Sect. A* **2008**, *64*, 112–122.

Received: May 30, 2011
Published online: November 16, 2011

